Elsevier Editorial System(tm) for Journal of Volcanology and Geothermal Research
Manuscript Draft

Manuscript Number:

Title: The Bero Volcanic Comples: Extension of The Paraná-Etendeka Igneous Province into SW Angola

Article Type: SI: CanonParana

Keywords: Angola; Paraná-Etendeka; basalt; quartz latite; geochemistry; stratigraphy

Corresponding Author: Prof. Julian Saville Marsh, PhD

Corresponding Author's Institution: Rhodes University

First Author: Julian Saville Marsh, PhD

Order of Authors: Julian Saville Marsh, PhD; Roger Swart, PhD

Abstract: Abstract
An extension of the Etendeka-Paraná Igneous Province into SW Angola occurs as minor basalt lavas, intrusive gabbro sheets, minor mafic dykes and thick sheets and lava flows (with minor pyroclastics) of quartz latite composition This suite outcrops along the eastern margin of the Cretaceous Namibe Basin in SW Angola. The quartz latites from one locality have been referred to informally as the Giraul volcanics but the name 'Giraul' has previously been used for Cretaceous conglomerates. We propose the name Bero Volcanic Complex for this suite of intrusive and extrusive rocks on the basis that the full compositional range of this diverse suite outcrop along the Rio Bero. Major and trace element compositions and Sr-, Nd-, and Pb-isotopic compositions indicate that the basalts and gabbros are equivalent to the high-Ti Khumib/Urubici and Pitanga types from the Etendeka and Paraná. The basalts underlie the quartz latites which are cut by mafic dykes some of which are compositionally equivalent to the Paranapanema lavas in the Paraná. Five different geochemical types of high-Ti quartz latite are recognised amongst the silicic volcanics, 3 of which have very close geochemical affinities to the Ventura, Sarusas, and Khoraseb types of the northern Etendeka. Their relative stratigraphic position in the Bero volcanic sequence is the same as in the Etendeka sequence and extend significantly the area over which these types were erupted. The two remaining types, Chinguau and High-Nb are not known from either the Etendeka or the Paraná provinces.

Suggested Reviewers: David Peate PhD
University of Iowa
david-peate@uiowa.edu
Expert on Paraná magmatism

Leila S Marques
University of Sao Paulo
Leila@iag.usp.br
Expert on Paraná magmatism

Chris Harris
University of Cape Town
chris.harris@uct.ac.za
Has published on Etendeka magmatism and has a knowledge of Paraná magmatsim

Piero Comin-Chiaramonti
University of Trieste
comin@univ.trieste.it
Has published widely on Cretaceous magmatism in South America and Angola

Cover letter

Here is my manuscript entitled:

Bero Volcanic Complex: Extension of the Paraná-Etendeka Igneous Province into SW Angola

This manuscript is intended for inclusion in the special issue of Journal of Volcanology and Geothermal Research on Paraná – Etendeka magmatism arising from the special session at the AGU Fall Meeting in December 2015.

The Figures have been embedded in the manuscript submitted for review, but data Tables have been submitted separately.

The following individuals might be able to provide reviews of the manuscript:

Prof David Peate, University of Iowa, david-peate@uiowa.edu

Prof L.S. Marques, University of Sao Paulo, Leila@iag.usp.br

Prof Tony Ewart, University of Queensland, a.ewart1@uq.edu.au

Prof Chris Harris, University of Cape Town, chris.harris@uct.ac.za

Prof Comin-Chiaramonti, university of Trieste, comin@univ.trieste.it

J.S . Marsh

Department of Geology

Rhodes University

Grahamstown

South Africa

Bero Volcanic Complex: Extension of the Paraná-Etendeka Igneous Province into SW Angola

J.S. Marsh and R.Swart

Highlights

- Bero Volcanic Complex is an extension of Paraná-Etendeka Province into S Angola
- Bimodal suite of high-Ti mafic lava and intrusions and high-Ti silicic volcanic rocks
- 3 quartz latite types equivalent to Sarusas, Ventura, Khoraseb types from Etendeka
- 2 new quartz latite types identified
- Volcanic stratigraphy consistent with that in Etendeka and Paraná

The Bero Volcanic Complex: Extension of the Paraná-Etendeka Igneous Province into SW Angola.

J.S. Marsh[a] and R.S Swart[b]

[a] Department of Geology, Rhodes University, Grahamstown, 6140 South Africa (corresponding author; e-mail: goonie.marsh@ru.ac.za)

[b] Blackgold Geosciences, P.O.Box 24287, Windhoek, Namibia. (e-mail: rogerswart@afol.com.na

Abstract

An extension of the Etendeka-Paraná Igneous Province into SW Angola occurs as minor basalt lavas, intrusive gabbro sheets, minor mafic dykes and thick sheets and lava flows (with minor pyroclastics) of quartz latite composition This suite outcrops along the eastern margin of the Cretaceous Namibe Basin in SW Angola. The quartz latites from one locality have been referred to informally as the Giraul volcanics but the name 'Giraul' has previously been used for Cretaceous conglomerates. We propose the name Bero Volcanic Complex for this suite of intrusive and extrusive rocks on the basis that the full compositional range of this diverse suite outcrop along the Rio Bero. Major and trace element compositions and Sr-, Nd-, and Pb-isotopic compositions indicate that the basalts and gabbros are equivalent to the high-Ti Khumib/Urubici and Pitanga types from the Etendeka and Paraná. The basalts underlie the quartz latites which are cut by mafic dykes some of which are compositionally equivalent to the Paranapanema lavas in the Paraná. Five different geochemical types of high-Ti quartz latite are recognised amongst the silicic volcanics, 3 of which have very close geochemical affinities to the Ventura, Sarusas, and Khoraseb types of the northern Etendeka. Their relative stratigraphic position in the Bero volcanic sequence is the same as in the Etendeka sequence and extend significantly the area over which these types were erupted. The two remaining types, Chinguau and High-Nb are not known from either the Etendeka or the Paraná provinces.

Keywords: Angola, Paraná-Etendeka, basalt, quartz latite, geochemistry, stratigraphy

1. Introduction

Two volcanic suites of Cretaceous age are associated with the Cretaceous on-shore Namibe Basin in SW Angola. The younger suite comprises Santonian-Campanian basanites and tephrites outcropping as small plugs, short dykes and extensive lava flows. The older suite is bimodal comprising abundant quartz latites and associated pyroclastic deposits and lesser volumes of basaltic lavas and associated intrusions (dykes, sheets). Only the silicic members of this suite have received prior attention. They were mapped and briefly decribed as 'granitic porphyries' by Carvalho (1961) who regarded them as Precambrian in age. Subsequently Alberti et al. (1992) published geochemical data for 3 samples of quartz latite collected along the roadpass above Rio Giraul. Referring to these as the 'Giraul Volcanics' these authors proposed a correlation with the Chapeco silicic rocks of the early Cretaceous Paraná-Etendeka Igneous Province. This correlation was subsequently confirmed by $^{39}Ar/^{40}Ar$ dating of plagioclase phenocrysts from one of the samples (TAG-2) by Renne et al.(1996).

During a reconnaissance stratigraphic mapping programme of the on-shore Namibe Basin under the auspices of Sonangol E.P. (Angola) and Statoil ASA (Norway) it became apparent that these early Cretaceous volcanic rocks outcrop extensively between latitudes 15.235^{o} S along the Rio Bero and 14.678^{o} S on the Rio Piambo. This prompted a regional geochemical and stratigraphic sampling programme of the volcanic rocks and associated intrusions, the results of which are reported here. A review of the stratigraphic nomenclature published by Carvalho (1961) indicates that the name 'Giraul' has been informally applied by him to a sequence of Upper Albian conglomerates. In addition the name has also been applied to a Precambrian pegmatite field by Goncalves et al.(2009, p36). As Carvalho's (1961) usage has priority it seems prudent to adopt a new name for the volcanic suite which is described comprehensively for the first time here. We propose the name Bero

Volcanic Complex for this igneous suite on the basis that the complete range of lithologies (quartz latites, mafic lavas, mafic intrusions, pyroclastic rocks) in the suite outcrops in the valley of the Rio Bero and its tributaries E of Namibe.

2. Distribution and Field Relationships

The Bero Volcanic Complex outcrops almost continuously in a partially fault-bounded block, up to 7 km wide and extending for over 65 km along the eastern margin of the Cretaceous Namibe Basin between Rio Bero and Rio Piambo (Figure 1). Along this eastern margin, the Bero Complex is frequently down-faulted against a variety of Precambrian basement lithologies but in places volcanic rocks overlie Precambrian schists unconformably, with an intervening aeolian sandstone veneer in the Bero area and a granite boulder conglomerate in the Rio Piambo and Manome areas. The maximum preserved thickness of the volcanic sequence is about 150-170m, the upper part having been eroded by a major Maastrichtian marine transgression and resulting shallow marine deposits locally overlies the sequence. Subsequent faulting has resulted in faulted contacts between the Bero Volcanic Complex and younger Cretaceous sediments lying to the west in many places. The volcanic sequence is also displaced by numerous faults, mostly coast-parallel, and with throws that are relatively small (metres to 10s of metres).

The Bero Complex is dominated by devitrified plagioclase-phyric lavas, occasional phyric pitchstones, and bedded pyroclastic rocks all of quartz latite composition. Basaltic lavas, which underlie the quartz latites, are confined to the Rio Bero area. Aeolian sandstones underlie and are discontinuously interbedded with these basalt lavas. Nowhere was the contact between the underlying aeolian sandstones and basement rocks observed.

In the Rio Giraul area and in all outcrops to the north basalt lavas are absent. However thin mafic dykes and larger gabbroic sheets intrude the quartz latites in the Rio Piambo area and along the western margin of the Bero Complex in the Manome area. The dykes provide evidence for the original presence of an upper sequence of basalt lavas, subsequently removed by erosion, overlying the quartz latites in the Bero Complex.

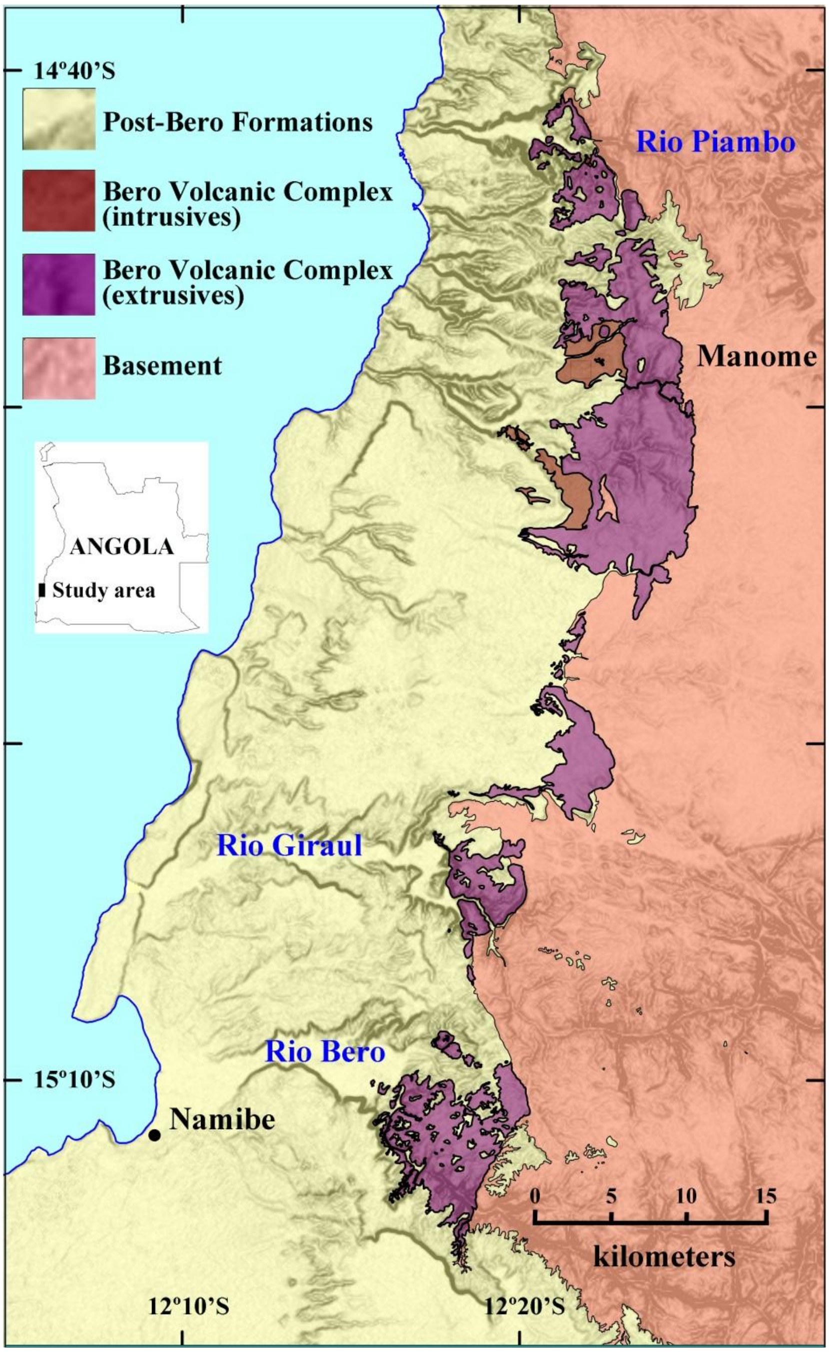

FIGURE 1 90mm width (one column width)

3. Volcanic Stratigraphy

Compared to the Etendeka of NW Namibia and the Serra Geral area of the Paraná the subdued topography, faulting, the virtual absence of basalts interbedded with quartz latite units, limited total preserved thickness, and extensive cover by younger Cretaceous sediments makes it difficult to comprehensively unravel the volcanic stratigraphy of the Bero Complex across its entire outcrop area.

3.1 Rio Bero area (15^{o}11.3’S; 12^{o}18.3’E)

Minor basaltic lavas and extensive quartz latites are exposed by numerous tributaries that have cut below the Maastrichtian planation surface mainly north of the main channel of the Rio Bero. Basalts occur in 3 closely spaced areas at about 15^{o}9.25’S; 12^{o}18.35’E. At least 4 flows are present and the sequence has a maximum preserved thickness of 40-50 m. Flows have rubbly tops infiltrated by red sand. Where exposed the basaltic lavas are underlain by an aeolian sandstone and in some places by thin yellow devitrified glassy airfall tuffs. Carvalho’s (1961) map of the area depicts these mafic lavas as post-Albian basanites, but major and trace element geochemistry and a K/Ar age (Cassignol-Gillot(1982) procedure) of 130.1±1.9 obtained for sample NBA-36 (G. Delpech, personal communication) indicates a clear correlation with high-Ti tholeiites of the Etendeka-Paraná province

Quartz laties overlie the basalts but are faulted down against the basalt sequence in several places. These relationships are exposed at only one locality, in the vicinity of 15^{o}8.950’S; 12^{o}17.580’E. The minimum thickness of the quartz latites is about 170m and geochemical evidence will later be presented for the presence of at least 3 flows in the sequence.

3.2 Rio Giraul area (15^{o}04.7’S; 12^{o}18.8’E)

In this area the Bero volcanic rocks occur in a block bounded by conspicuous faults. To the E the sequence is faulted down against basement schists whereas on the W a thick sequence of coarse Cretaceous conglomerates are faulted down against the Bero volcanic sequence. This contact is beautifully exposed on the roadpass above the Rio Giraul on the Lubango-Namibe highway. The volcanic sequence comprises two quasi-horizontal quartz latite sheets with a combined maximum thickness of 140-150m. The base of the sequence is not exposed at Rio Giraul but 7km to the north a quartz-latite sheet overlies coarse cross-bedded sandstones and grits whose base is not exposed and a further 19km to the north the basal quartz latite sheet overlies Precambrian granitic basement. At the Rio Giraul the eroded upper surface of the Bero sequence is overlain by Maastrichtian and younger sedimentary sequences.

3.3 Manome area (14^{o}49.5'S; 12^{o}23.5'E)

Two quartz latite sheets characterize this area as exposed in the E-W gorge just S of Manome beacon. The volcanic sequence is down faulted against Precambrian basement rocks to the east and its western margin against the younger Cretaceous sedimentary succession is also fault banded in part. The volcanic sequence is displaced along a number of N-S trending faults with small throws. At the western end of the gorge the lower quartz latite overlies Precambrian granite outcropping in the river bed. As in other areas the quartz latite succession has been planed off by the major Maastrichtian marine incursion on which a remnant of the Maastrichtian sediments is preserved at Manome beacon as well as at a number of localities further N.

3.4 Rio Piambo area (14^{o}42.1'S; 12^{o}21.4'E)

The northernmost extent of Bero Volcanic rocks outcrop in the gorge of Rio Piambo. Again the Bero sequence is down faulted against Precambrian basement rocks along the eastern margin of the outcrops and overlain by gypsum and succeeding younger Cretaceous sedimentary rocks. There is evidence of considerable erosional topographic relief in the Bero sequence prior to the Cretaceous sedimentation with the large area of gypsum measuring 2 X 0.8 km surrounded by, and nestled amongst, quartz latite. A number of valleys filled with coarse Albian conglomerates have also been carved into the Bero sequence. Volcanologically this is a complex area with clear evidence of short lava flows and associated red and cream-coloured airfall pyroclastic deposits interlayered with the lavas. In other places there is evidence of thick stacked rheoignimbritic sheets similar to the Manome and Rio Giraul areas. The base of the volcanic sequence is exposed in a number of places and is characterized by a granite boulder conglomerate infiltrated by volcanic ash and overlain by laminated airfall material which in turn is overlain with an irregular contact by glassy lava, now largely devitrified. However, the sequence is displaced by numerous small faults and lateral continuity of units is difficult to determine.

4. Petrography

4.1 Mafic rocks

Basaltic lavas and intrusive dykes are petrographically very similar. All are aphyric and textures range from holcrystalline intergranular through intersertal to hyalopilitic with grains size of the dominant plagioclase laths ranging from 0.2 to 0.6 mm in length. Mafic phases are granular augite and opaque oxides. When present glass is strongly devitrified and varies from brown glass crowded with crystallites and microlites to oxidised opaque material. The gabbroic sheets are holocrystaline subophitic and more coarse grained and dominated by slender euhedral plagioclase laths ranging up to 1.3 mm partially enclosed by anhedral blocky augite ranging in size up to 3mm. Minor olivine, variably serpentinized is present in several specimens. Opaque oxides, blocky magnetite and slender ilmenite needles are ubiquitous. The evolved gabbro (NBA-139) is inequigranular seriate and hypocrystalline. Strongly zoned blocky plagioclase with thick alkali feldspar rims dominates. Slender euhedral augite laths up to 4 cm long are common. Quartz occurs in interstitial areas as do pools of devitrified glass crowded by small blocky feldspar grains.

4.2 Quartz latites

A number of petrographic features are common to all Bero quartz latites. Significant alteration /oxidation is a feature of most outcrops but some black, glassy pitchstones are present. All quartz latites are strongly plagioclase-phyric (with phenocrysts ranging up to 8mm) and are characterized by an anhydrous primary mafic mineralogy (pyroxenes, Fe-Ti oxides). A devitrified groundmass is ubiquitous and ranges from grey glass crowded with microlites and crystallites with rod-like and whispy habits, to holocrystalline felsitic intergrowths of feldspar and quartz of variable grain size. The grain size of the devitrified groundmass appears to reflect both the thickness of the quartz latite flow and where within the flow the sample was collected. In all respects the Bero quartz latites have all the petrographic features of the Etendeka and Paraná quartz-latites described in detail by Ewart et al. (1998), Ewart et al.(2004b) and Bellieni et al. (1986). In Section 4.4 a number of quartz latites types are recognised in the Bero suite on the basis of geochemistry and a question arises whether these types have specific petrographic characteristics. Although all types have similar petrography, the Chinguau type is characterized by the ubiquitous occurrence of fritted plagioclase in the phenocryst population. Fritting may be a feature of complete grains or may occur in rims of grains. Fritting was not observed in phenocrysts of other types.

5. Geochemistry

5.1 Analytical Methods

Major and trace elements (Nb, Zr, Y, Sr, Rb, Zn, Cu, Ni, Co, Cr, V, Ba, Sc, La, Ce, Nd) were determined by wave-length X-ray Fluorescence Spectrometry (XRF) at Rhodes University using methods described in detail by Duncan et al. (1984). The Bero data will be compared with data from the

Etendeka Igneous Province (Marsh et al., 2001) and it is important to note that all the Etendeka rocks were either analyzed in the XRF laboratory at Rhodes University or the University of Cape Town with repeated checks to eliminate any interlaboratory biases. The Bero XRF analyses are thus directly comparable to the Etendeka data. A subset of Bero samples were analysed for REEs, Th, U, Hf, Ta and Pb and Sr- Nd- and Pb-isotopes in the MC-ICP-MS analytical facility at the University of Cape Town following procedures described in detail by Harris et al. (2015). A growing body of modern Ar-Ar and particularly U-Pb dating studies (Thiede and Vasconcelos, 2010; Janasi et al., 2011; Pinto et al.,2011; Florisbal et al., 2014) suggest that mafic and silicic volcanics in the Paraná were emplaced over a short period between 134 Ma and 135 Ma. Thus all initial ratios, both new data for Bero rocks and those of the Paraná-Etendeka province published previously, have been recalculated at 134.5 Ma and for $^{87}Sr/^{86}Sr$ the recommended decay constant for $^{87}Rb = 1.397 \times 10^{-11}$ a^{-1} (Villa et al., 2015) has been adopted. Isotopic data are presented in Figure WWW where they are compared to published data from the Etendeka and Paraná. For Pb-isotopes measured ratios rather than initial ratios have been plotted as the lack of U, Th, or Pb concentration data for over two thirds of the Paraná and Etendeka samples prevent initial ratios being calculated. Analyses for selected samples are presented in Table 1 and the complete geochemical dataset is available in Supplementary Table. Concentration data plotted on variation diagrams has been normalised to 100% free of volatiles.

5.2 Overall compositional variation in the Bero rocks

Figure 2 illustrates the bimodal nature of the Bero igneous suite with mafic rocks spanning the fields of basalt and basaltic andesite and the silicic rocks plotting close to the junction of the fields of rhyolite, dacite and trachydacite. This is very similar to the spread of compositions found in the Etendeka igneous province of Namibia, and we follow the nomenclature adopted there by referring to the mafic rocks as ‘basaltic’ and the silicic rocks as ‘quartz latite’ (see Marsh et al.,2001 for discussion on this nomenclature). Apart from an evolved intrusive gabbro (NBA-139) the Bero mafic rocks plot within the field for Etendeka basaltic rocks. Bero quartz latites also overlap with the Etendeka field except for a small group of samples which plot at much higher Na_2O+K_2O in the trachydacite field. These all belong to the High-Nb geochemical type which is defined in a later section. It is noticeable that there are no equivalents of the Etendeka latites in the Bero suite.

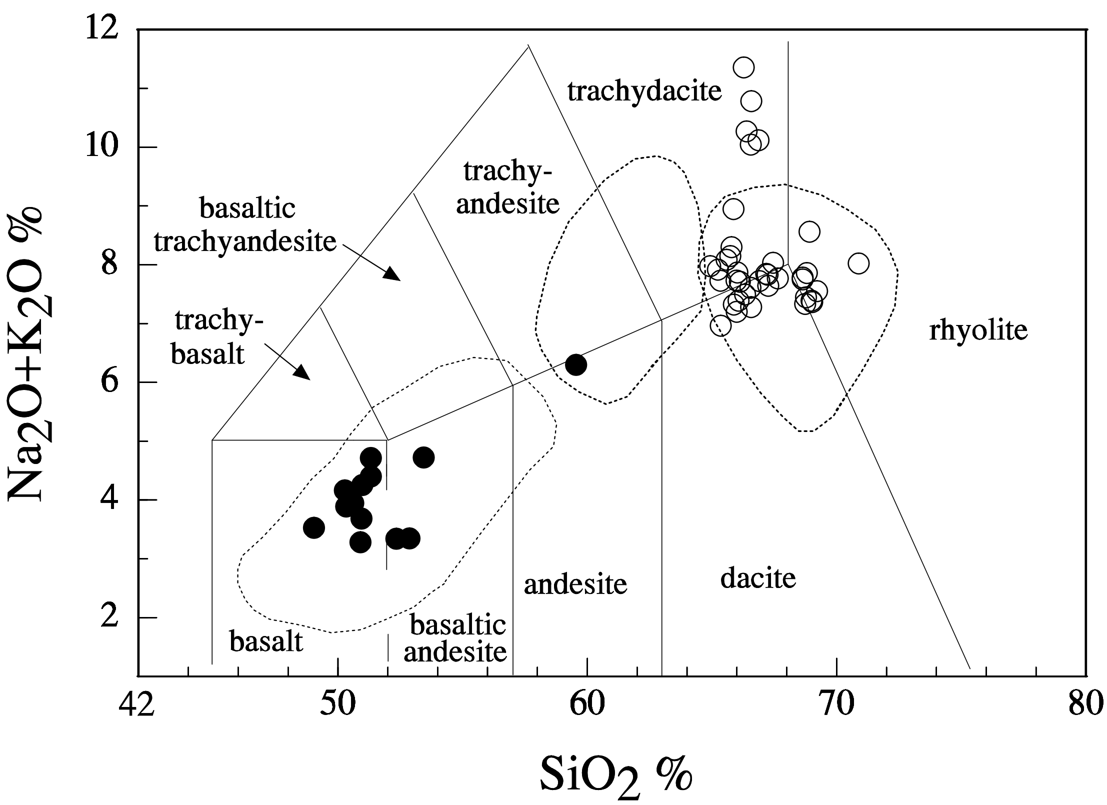

FIGURE 2 90mm width (one column width)

5.3 Mafic rocks

In the Etendeka the basaltic rocks comprise the high-Ti Khumib lavas and the low-Ti Tafelberg, Albin, Horingbaai, Esmeralda and Kuidas lavas and intrusions. Marsh et al.(2001) used a plot of Sr vs TiO_2 and the Ti/Y ratio to discriminate between the high- and low-Ti groups and showed that a plot of

Zr/Y vs Mg# can be used to differentiate amongst the low-Ti types. In the Parana there are four high-Ti types, the Paranapanema, Pitanga, Ribeira and Urubici types (Peate, 1997). The Urubici type dominates in the south along the Sera Geral escarpment and is equivalent to the Khumib type (Peate, 1997; Marsh et al., 2002). In stratigraphic order, the Ribeira, Pitanga, and Paranapanema types form thick sequences of flows throughout the central and northern parts of the Paraná basin with the Pitanga and Parapanema types each having erupted volumes about 20% of the total (Peate,1997), far greater than the Urubici type. In terms of stratigraphy the Urubici lavas are interbedded with low-Ti basalts and predate the silicic eruptives whereas other high-Ti types appear to be younger than the silicic volcanism. Distinction between the different high-Ti types can be made on the basis Ti/Y and Fe/Ti and Fe/Sr ratios with the Ribeira and Paranapanema having a close geochemical affinity (Peate, 1997).

Figure 3 shows the Bero mafic rocks plotted on discrimination diagrams prepared from databases of many hundreds of analyses from the Etendeka and Paraná provinces. Bero mafic rocks fall into two groups: the bulk of the lavas and intrusions having higher TiO_2 > 3% and 3 intrusions having lower TiO_2 < 3%. The higher-Ti group overlaps with the field for the Khumib/Urubici type in the TiO_2 – Sr

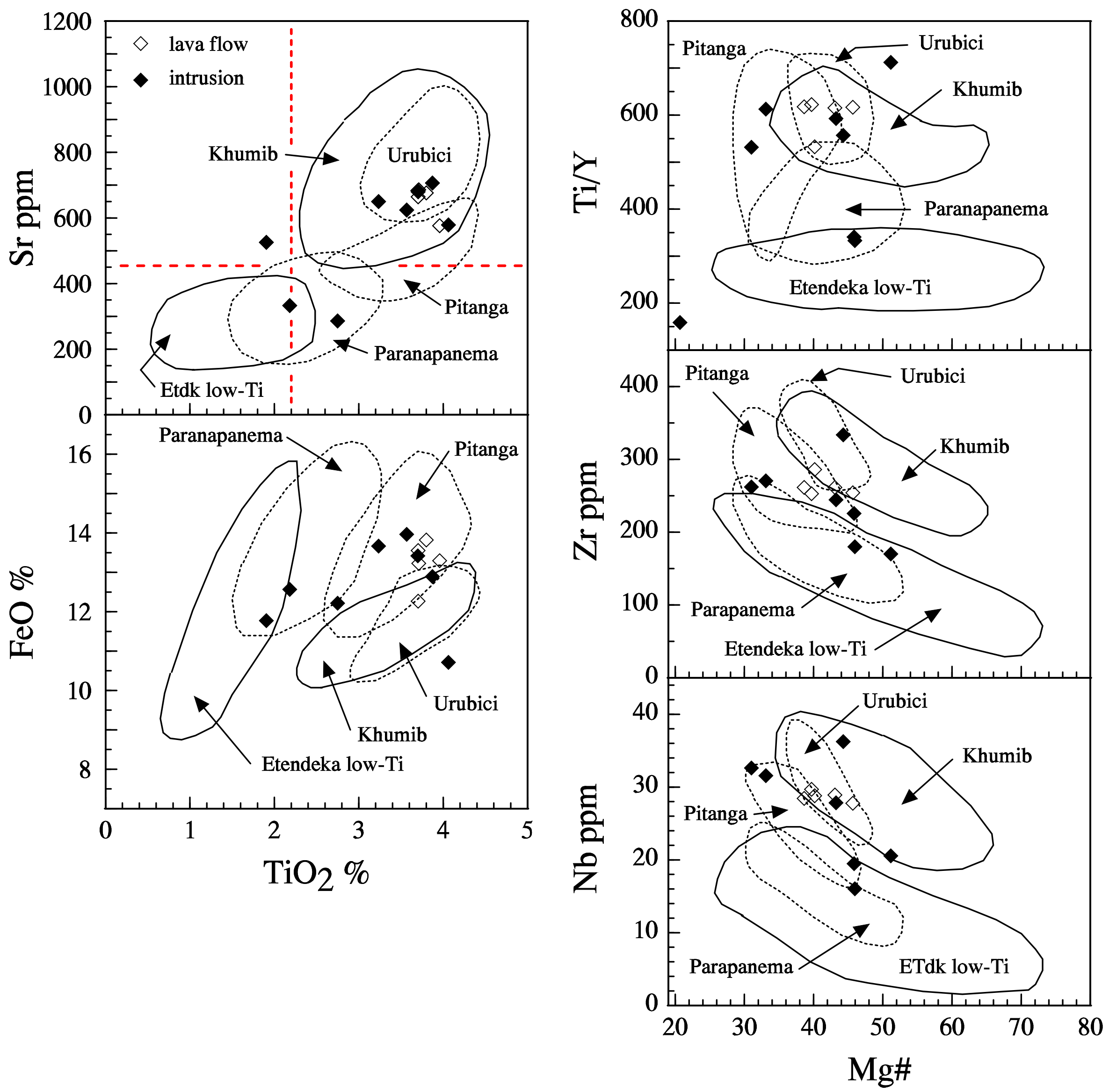

FIGURE 3 Across two columns

plot (Fig 3). Peate (1997)used Ti/Fe ratios to distinguish between different high-Ti types in the Paraná and the Bero rocks are compared with fields for these types in FeO vs TiO_2 (Fig. 3). The higher-Ti samples scatter across the fields of Uribici and Pitanga types with most concentrating in the Pitanga field as a consequence of their higher FeO.

Of the three lower-Ti samples (TiO2 , 3%) one (NBA-139) is an evolved gabbro with Mg# = 20, Ni and Cr concentrations < 3ppm, V = 22 ppm, low Ti/Y (<200) and very high Zr, Nb, P, Ba, and Y. Such features reflect extensive fractional crystallization involving mafic silicate phases and Fe-Ti oxides, making it impossible to determine its original magmatic provenance. The other two samples are dykes intruding quartz latite and they have close geochemical affinities to the Paranapanema type. These dykes presumably fed Paranapanema lava eruptions that once overlay the quartz latites, but which are no longer preserved in the Namibe basin. This implied stratigraphic position of the Paranapanema type relative to the quartz latites is consistent with that in the Paraná basin. The juxtaposition of Africa and South America at 135 Ma places the Namibe basin dykes adjacent to known occurrences of the Paranapanema lavas in Brazil.

Isotopic data are plotted in Figure 5 where the Bero data is compared to fields for various mafic and silicic types from the Paraná and Etendeka. For Pb-isotopes measured values have been plotted because many Paraná and Etendeka samples lack either U, Th, or Pb concentrations, precluding calculation of initial ratios for over two thirds of samples for which Pb-isotopes have been determined.

The two Bero mafic samples which, on the basis of whole-rock compositional data have been identified as being equivalent to the Khumib/Urubici type, have Sr- and Nd-isotopic compositions comparable to the field of Urubici-Khumib, Pitanga and Paranapanema types. These samples have measured ^{206}Pb/^{204}Pb > 18 which is much higher than the bulk of Khumib/Urubici samples from Etendeka-Paraná, but which is a feature of the uppermost Unit E of the Urubici sequence in the Paraná (Peate et al., 1999). These high ^{206}Pb Khumib flows are not currently known from the Etendeka.

5.4 Silicic Rocks

In the Etendeka silicic rocks interbedded with mafic lavas comprise 6 low-Ti and 5 high-Ti quartz latite types (Khoraseb, Ventura, Sarusas, Elliott and Naudé types) as well as 5 latite types based on geochemistry, petrography, and stratigraphy (Marsh et al.,2001). All high-Ti quartz latites and one low-Ti type (Fria quartz latite)occur in the northern Etendeka region. In the Paraná low-Ti Palmas 'rhyolites' can be subdivided into 5 sub groups and the high-Ti Chapecó 'rhyolites' comprises 3 sub groups (Ourinhos, Guarapuava, and Tamarana - Garland et al.,1995; Nardy et al.,2008). These subdivisions are based on stratigraphy, petrography and particularly whole rock geochemistry. Milner et al.(1995) and Marsh et al.(2001) showed that many of the Etendeka and Paraná types can be correlated based on whole-rock geochemistry.

Because of the implications for the size of magma systems developed along continental rift margins (Bryan et al., 2010) it is important to determine whether any of the Etendeka and Paraná quartz latite chemical types are represented in the Bero suite. Alberti et al. (1992) have already identified the presence of the Chapecó type of the Paraná in the Bero suite on the basis of 3 samples collected from a single flow just N of the Giraul River.

Data from our larger collection of quartz latites (39 samples collected from all outcrop areas are compared to fields for Etendeka quartz latites on geochemical discrimination diagrams (partly from Marsh et al.,2001) in Figure 4. Additional comparison of some interelement ratios are presented in Table 2. It is clear that all Bero quartz latites classify as high-Ti and that quartz latites with close geochemical affinities to the Ventura, Sarusas, and Khoraseb types of the northern Etendeka are present in the Bero suite, although there are slight compositional differences. The Sarusas samples from the Bero have slightly higher FeO and lower Zr (hence slightly lower Zr/Nb) compared to the Sarusas suite from the Etendeka. The Ventura samples in the Bero are slightly enriched in HREE and Y compared to the Etendeka suite, hence the differences in Ti/Y and La/Yb in Table 2.

In addition two further quartz latite types present in the Bero suite. These are the Chinguau type with high SiO_2, variable FeO and TiO_2, similar Nb, and low P_2O_5 and Zr compared to the Ventura-

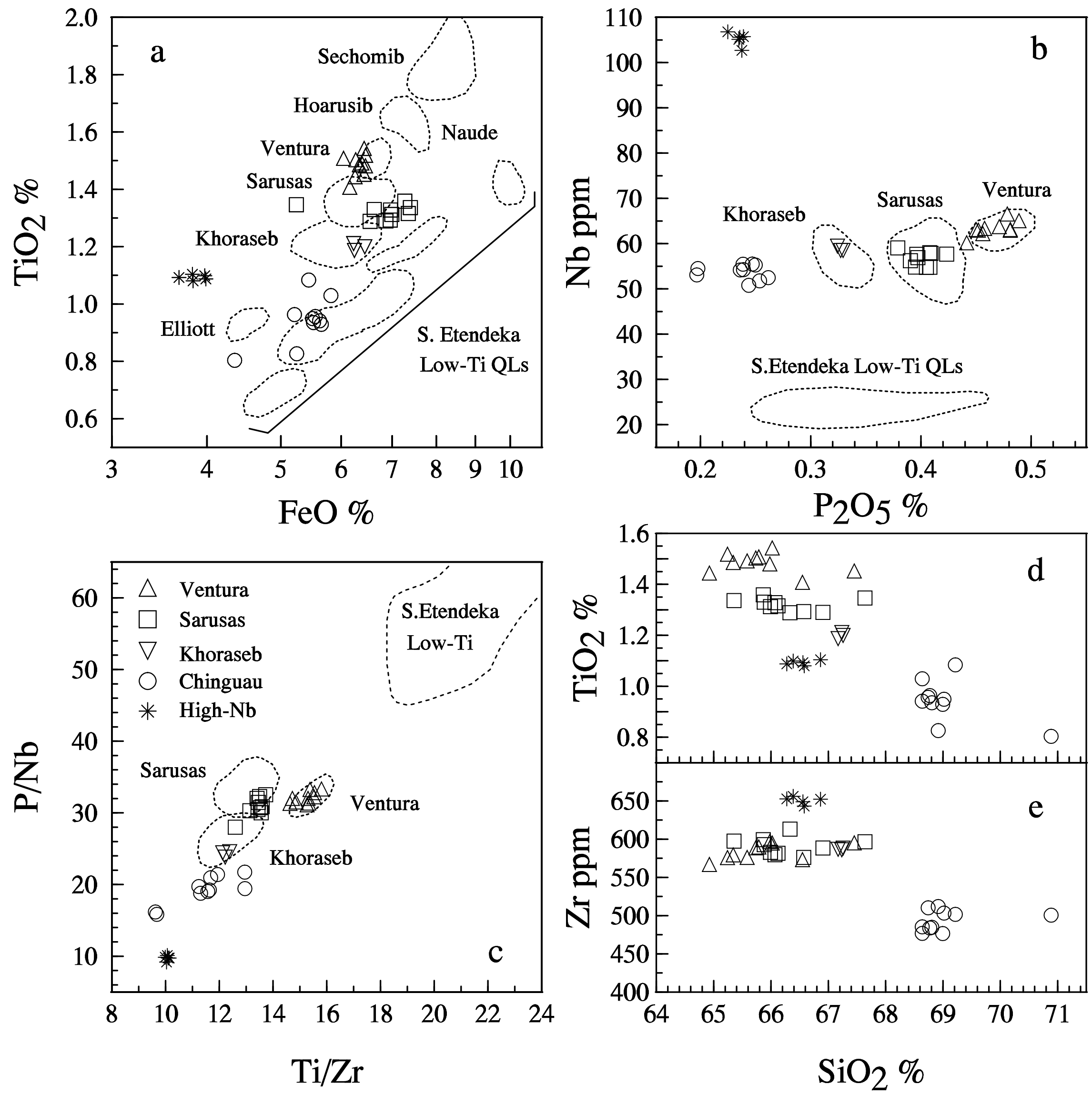

FIGURE 4 Across two columns

Sarusas-Khoraseb suite. The other type, the High-Nb type, has distinctly high Nb (> 100 ppm), Al_2O_3, Zr, Rb, Th, total alkalies, and lower P_2O_5, FeO and Sr compared to the other types (Figures 2, 4). The High-Nb type plots in the trachydacite field on the TAS diagram (Figure 2 The variations within and between the Ventura, Sarusas, and Khoraseb types has been described by Ewart et al. (2004b) and those descriptions apply equally to the Bero rocks. In general there are general trends with increasing SiO_2 of decreasing TiO_2 (Figure 4) Al_2O_3, FeO, P_2O_5, Sr, and increasing Rb, Th, Pb. Concentrations of other major and trace elements are scattered. The high Nb type is frequently displaced to higher or lower concentrations for its SiO_2 content compared to the general trend (Figure 4). Quartz latites with compositional characteristics of the Chinguau and High-Nb types have not previously been reported from the Etendeka nor the Paraná.

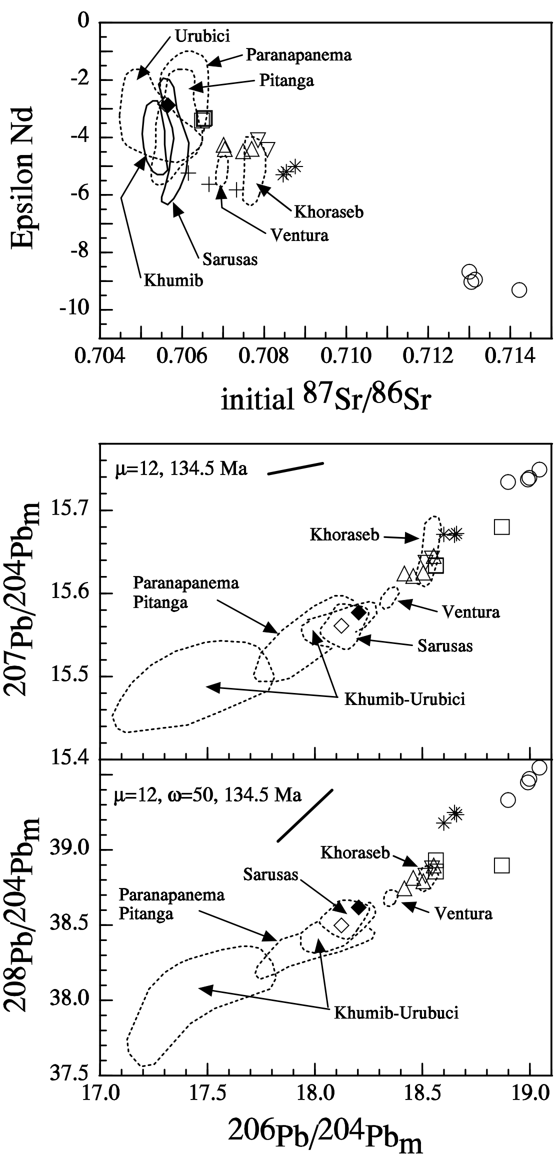

FIGURE 5 (One column width – 90 mm)

Isotopic data for the Bero quartz latites where they are compared to fields for some of the high-Ti quartz latite types from The Paraná and northern Etendeka (Figure 5). In the Sr-Nd isotope correlation diagram there is a close (but not exact) correspondence between the Bero Ventura and Khoraseb samples and the Etendeka-Paraná fields for these types. The Bero Sarusas samples plot at slightly higher initial $^{87}Sr/^{86}Sr$ (about 0.7065) than their Etendeka-Paraná equivalents. The High-Nb and especially the Chinguau type have higher initial $^{87}Sr/^{86}Sr$ and lower epsilon Nd values, the latter approaching the radiogenic Sr-isotopic compositions of the Etendeka low-Ti types. The 3 'Giraul' samples analysed by Alberti et al. are not shown on Figure 5 as they give no technical analytical details for their isotope analyses and no Sm/Nd data necessary to calculate initial Nd isotopic ratios. However their data deserve comment . Calculated initial $^{87}Sr/^{86}Sr$ ratios for the 3 'Giraul' samples range from 0.7062-0.7073 and overlap with the much narrower range for the Bero Sarusas type reported here. However calculated initial Nd-isotopic compositions using an estimated Sm/Nd = 0.195 (typical of the Sarusas type) give epsilon Nd values 2 units lower than our data. There is no explanation for this discrepancy. Measured Pb-isotopic compositions in the Bero rocks show good agreement for the Khoraseb type with the Etendeka-defined field but a slight mismatch for the Ventura and a large mismatch for the Sarusas type. The High-Nb and Chinguau types have more radiogenic Pb-isotopic compositions consistent with higher initial $^{87}Sr/^{86}Sr$ and lower epsilon Nd.

In evaluating the significance of the apparent differences between the isotopic compositions of the Bero quartz latites and those from the Etendeka/Paraná, it must be born in mind that isotopic data for the latter are very few compared to data available for mafic rocks. For example, there are only 2 Ventura samples from the Etendeka for which Sr-, Nd-, and Pb-isotopic analyses are available (versus 4 Bero samples !). The combined samples of the Sarusas-Guarapuava type for which data is available numbers only 7 for Sr- and Nd-isotopes and 6 for Pb-isotopes, despite the large area over which these types occur, particularly in the Paraná. The possibility exists that a more comprehensive database of isotopic data for quartz latite types in the Etendeka and Paraná might render the mismatches reported here less significant.

6. Geochemical Stratigraphy

To further strengthen the quartz latite correlations it is important to take into account stratigraphy. The northern Etendeka latite and quartz latite types have a stratigraphic distribution which from oldest to youngest is: Sechomib-Hoarusib-Ventura-Khoraseb-Sarusas(with Elliott interbeds)-Naude (Figure 6 and Marsh et al., 2001). The stratigraphic distribution of the quartz latites types at different localities across the Bero outcrop area is also shown in Figure 6. Although not present at all localities, the stratigraphic distribution of the Ventura, Khoraseb and Sarusas types is consistent across the area and with their relative stratigraphic position in the Etendeka. Additionally, the Chinguau type is younger that the Ventura, but where the latter is absent the Chinguau lies on the basal mafic lavas (Bero area) or directly on pre-volcanic conglomerates (Piambo area). The High-Nb type, known only from the Piambo area, lies between the Chinguau and Sarusas type but its age relative to the Khoraseb type is unknown.

7. Petrogenesis

The petrogenesis of the Etendeka-Paraná high- and low-Ti silicic volcanic rocks has been exhaustively explored in a number of studies with little consensus between rather diverse petrogenetic proposals made by different researchers. These include: derivation by AFC processes from basaltic magmas; derivation by fractional crystallization from associated basalt; being melting products of a variety of crustal lithologies or associated underplated basalt; being products of magma mixing; and various combinations of these (Erlank et al., 1984; Belieni et al., 1986; Piccirillo et al., 1988; Garland et al., 1996; Harris and Milner, 1997; Ewart et al., 2004b with the latter reference containing an extensive discussion and review).

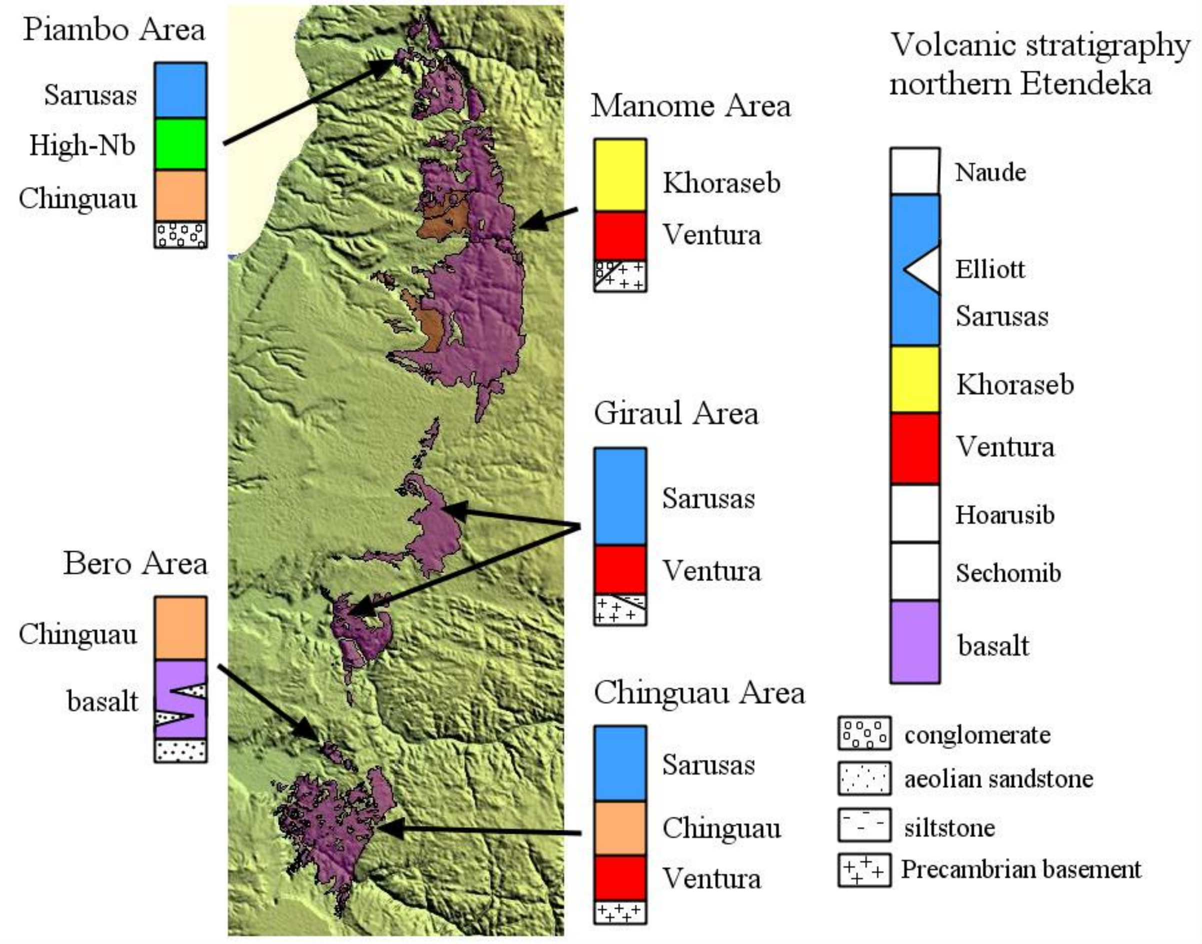

FIGURE 6 (across two columns)

This diversity of opinion reflects a number of important factors. Firstly the eruption sites of the silicic volcanics are unknown and, apart from minor Chapecó dykes in the Ponta Grosso dyke swarm in Brazil (Piccirillo, et al.,1990), presumably were located close to the original continental rift and now lie offshore. Second, the high-Ti - low-Ti geochemical provinciality of both mafic and silicic mama types suggests a fundamental petrogenetic link between the mafic and silicic magmas. Third, the volumes of many of the silicic magma types are huge and the current work extends significantly the area over which the Ventura and Khoraseb-Ourinhos types were erupted (see Marsh et al., 2001). The Etendeka-Paraná volcanic province as a whole was a giant, complex, magma system involving mafic magmas from different mantle sources emplaced through and possibly interacting with crustal lithologies spanning different crustal provinces. Under such constraints detailed petrogenetic modelling relies on many assumptions rendering the significance of the results somewhat uncertain.

7.1 Sarusas, Khoraseb and Ventura quartz latites

For these types the Bero data add very little to petrogenetic models presented and discussed by Ewart et al. (2004b). The presence of the Ventura type in the Namibe basin extends the area over which it occurs significantly and should perhaps be removed from the classification as part of the small-volume suite as proposed by Ewart et al.(2004b). The slight differences in LREE/HREE (and ratios like Ti/Y), compared to the Etendeka may suggest slight geochemical heterogeneity in the source rocks of this type or the end-members in more complex petrogenetic models (AFC, magma mixing). The most important geochemical difference exhibited by the Sarusas type in Angola is the isotopic composition of Sr and especially Pb.

On the basis of extensive modelling of a variety of processes involving major and trace elements and isotopes, Ewart et al.(2004) favoured derivation of the Khoraseb type from the Urubici-Khumib type by AFC processes with an assimilant equivalent to middle crust with very low R (=0.08) and F, i.e. crystallization dominating over rate of assimilation. The Sarusas type being slightly more mafic and with lower Sr- and Pb-isotopes was derived from the Khoraseb by mixing with basaltic magma into the Khoraseb magma pool, or by a continuation of the AFC process producing the Khoraseb with further assimilation of the more mafic restite of the middle-crust assimilant. These models might appear to be inconsistent with Pb isotope data which, in the Bero suite, shows an overlap in

$^{206}Pb/^{204}Pb$ of the Khoraseb and Sarusas types. If the mafic component in the mixing/assimilation models has very low Pb/Sr a significant lowering of $^{87}Sr/^{86}Sr$ can be achieved with very slight shift in $^{206}Pb/^{204}Pb$. For example, using the initial isotope ratios and element concentrations in Table 1 simple mixing of Khoraseb composition NBA-129 (Pb/Sr = 0.064) with high-Ti basalt NBA-36 (Pb/Sr = 0.0069) results in a mixture with $^{87}Sr/^{86}Sr$ = 0.70655 (equivalent to average Sarusas type in the Bero suite) and $^{206}Pb/^{204}Pb$ = 18.257 (slightly lower in comparison to $^{206}Pb/^{204}Pb$ = 18.286 in the parental Khoraseb composition). This calculation, using actual compositions, emphasises that overlap in Pb-isotopic compositions of the Sarusas and Khoraseb Pb types in the Bero data need not be an obstacle to the general models proposed by Ewart et al. (2004b) for the Etendeka-Paraná suite. We, however, do not propose that our simple calculation proves this particular petrogenetic model. What is clear is that a more comprehensive isotopic dataset, particular for Etendeka and Paraná silicic types is required to evaluate relationships between the quartz latite types from the different regions and their petrogenesis. Even then the challenges outlined in Ewart et al.(2004b) that frustrate the elimination of possible petrogenetic models still remain.

7.2 The Chinguau and High Nb quartz latites.

These appear to be small-volume eruptives relatively early in the quartz latite sequence (Fig 6). The Chinguau type shares some compositional characteristics with other high-Ti quartz latites (e.g. high Ba, Zr, Nb, Zr/Nb, La/Yb, Eu/Eu*, Ce/Pb) but have radiogenic Sr and Pb isotopic compositions and low epsilon Nd overlapping with data for low-Ti quartz latites (Fig 4 and Table 2), indicating the presence of a significant crustal component. In terms of the AFC models favoured by Ewart et al. (2004b) for the origin of the high-Ti quartz latites from the northern Etendeka these data imply a much larger rate of assimilation to crystallization (the R factor) for the Chinguau type than required for the other quartz latites, or the involvement of an assimilant with more radiogenic $^{87}Sr/^{86}Sr$ and Pb isotopic composition (but lower $^{143}Nd/^{144}Nd$). However, a higher R produces trace element misfits, particularly for Ba and Nb and we propose that the geochemical features of the Chinguau type reflects involvement of an assimilant which is isotopically different to that involved in the petrogenesis of the other quartz latites.

In contrast, the High-Nb type maintains the compositional and isotopic flavour of the other high-Ti quartz latites, but also has unusually high Nb, and high and distinctive Na_2O+K2O, Ti/Fe, Rb/Sr and low Zr/Nb and P/Nb. In terms of critical geochemical features the High-Nb type shares nothing with low-Ti quartz latites. On this basis the petrogenetic models advanced by others for the high-Ti quartz latites are probably relevant to the high-Nb type, but involve a crustal component which is more alkaline and syenitic (to account for the higher K_2O, Al_2O_3, Rb, Rb/Sr). Various syenitic rocks occur in ring complexes emplaced more-or-less contemporaneously with the flood volcanism in the Etendeka (Damaraland complexes – Martin et al.,1960; Woolley, 2001), Brazil (Ponta Grossa Arch and Serra do Mar – Amaral et al., 1967; Woolley, 1987), and in Angola (Lapido-Loureiro, 1973; Woolley, 2001). This indicates the limited availability of syentic liquids which could potentially be involved in open-system petrogenesis of the small-volume High-Nb quartz latite although there is currently no known occurrence of syenites of appropriate age in the Rio Piambo area.

8. Summary

Eroded remnants of the Paraná-Etendeka Igneous Province occur as the Bero Volcanic Complex at the base of the Cretaceous on-shore Namibe Basin in SW Angola. The Bero Complex is dominated by quartz latite rheoignimbrite sheets and lava flows overlying geographically restricted minor basalt lava flows, some airfall pyroclastic deposits, and intrusive mafic dykes and gabbroic sheets. Geochemically all these rocks are high-Ti in the context of the Paraná-Etendeka province. The basaltic lavas and majority of mafic intrusions are geochemical equivalents of the Khumib/Urubici and Pitanga mafic types in Paraná-Etendeka province. Two dykes cutting the quartz latites are equivalent to the Paranapanema mafic lavas in Brazil, implying that such lavas probably overlay the quartz latites but are now no longer preserved. Five geochemical types are recognised in the quartz latites, three having very close geochemical affinities to the Sarusas, Khoraseb, and Ventura types from the northern Etendeka region. These types have the same stratigraphic relationships to each other as in the Etendeka. Two new types are the Chinguau and High-Nb types. The widespread Chinguau type shares compositional features with both the high-Ti and low-Ti quartz latites. The High-Nb type is aerially restricted and has no low-Ti characteristics. The generalised petrogenetic AFC models advocated by Ewart et al. (2004) are relevant to all the Bero quartz latites with the assimilant in generating the Chinguau types being characterized by radiogenic Sr- and Pb- and nonradiogenic Nd-isotopic compositions. It is proposed that the assimilant in the generation of the High-Nb type is syenitic in character.

Acknowledgements

This research was partially funded by the National Research Foundation (NRF) of South Africa through a grant No. 85340 to JSM. Logistic support for field work in Angola was provided by Staoil ASA and Sonangol E.P.. The funding sources had no other involvement in this research and any opinion, findings, and conclusions in this paper are those of the authors. JSM wishes to thank Dave Peate for generously making his database of Paraná analyses available for the preparation of several figures.

References

Alberti, A., Piccirillo, E.M., Bellieni, G., Civetta, L., Comin-Chiaramonti, P. and Morais, E.A.A., 1992. Mesozoic acid volcanics from southern Angola: Petrology, Sr-Nd isotope characteristics and correlation with the acid stratoid volcanic suites of the Paraná basin (south-eastern Brazil). European Journal of Mineralogy, 4, 597-604.

Amaral, G., Bushee, J., Cordani, U.G., Kawashita, K. and Reynolds, J.H., 1967. Potassium-argon ages of alkaline rocks from southern Brazil. Geochimica et Cosmochimica Acta, 31, 117-142.

Bellieni, G., Comin-Chiaramonti, P., Marques, L.S., Melfi, A.J., Nardy, A.J.R., Papatrechas, C., Piccirillo, E.M., Roisenberg, A. and Stolfa, D., 1986. Petrogenetic aspects of acid and basaltic lavas from the Paraná Plateau (Brazil): Geological, mineralogical and petrochemical relationships. Journal of Petrology, 27, 915-944.

Bryan, S.E., Ukstins Peate, I., Peate, D.W., Self, S., Jerram, D.A., Mawby, M., Marsh, J.S. and Miller J.A., 2010. The largest volcanic eruptions on Earth. Earth Science Reviews, 102, 207-229.

Carvalho, G.S. de, 1961. Geologia do deserto de Moçâmedes (Angola). Junta de Investigações do Ultramar, Lisboa, 227 pp.

Cassignol, C. and Gillot, P.Y., 1982. Range and effectiveness of unspiked potassium argon dating: Experimental groundwork and applications. In: Odin, G.S. (Ed.) Numerical Dating in Stratigraphy, John Wiley, New York, 159-179.

Duncan, A.R., Erlank, A.J. and Betton, P.J., 1984. Appendix 1: Analytical techniques and database descriptions. Geological Society of South Africa Special Publication, 13, 389-395.

Erlank, A.J., Marsh, J.S., Duncan, A.R., Miller, R. McG., Hawkesworth, C.J., Betton, P.J. and Rex, D.C., 1984. Geochemistry and petrogenesis of the Etendeka volcanic rocks from SWA/Namibia. Geological Society of South Africa Special Publication, 13, 195-245.

Ewart, A., Milner, S.C., Armstrong, R.A. and Duncan, A.R. (1998) Etendeka volcanism of the Goboboseb Mountains and Messum Igneous Complex, Namibia. Part II: Voluminous quartz latite volcanism of rhe Awahab magma system. Journal of Petrology, 39, 227-253.

Ewart, A., Marsh, J.S., Milner, S.C., Duncan, A.R., Kamber, B.S., and Armstrong, R.A., 2004a. Petrology and geochemistry of early Cretaceous bomodal continental flood volcanism of the NW Etendeka, Namibia. Part 1: Introduction, mafic lavas and re-evaluation of mantle source components. Journal of Petrology, 45, 59-105.

Ewart, A., Marsh, J.S., Milner, S.C., Duncan, A.R., Kamber, B.S. and Armstrong, R.A., 2004b. Petrology and geochemistry of Early Cretaceous bimodal continental flood volcanism of the NW Etendeka, Namibia. Part 2: Characteristics and petrogenesis of the high-Ti latite and high-Ti and low-Ti voluminous quartz latite eruptives. Journal of Petrology, 45, 107-138.

Florisbal, L.M., Heaman, L.M., Janasi, V. de A. and Bitencourt, M. de F., 2014. Tectonic significance of the Florianópolis Dyke Swarm, Paraná-Etendeka magmatic province: A reappraisal based on precise U-Pb dating. Journal of Volcanology and Geothermal research, 289, 140-150.

Garland, F., Hawkesworth, C.J., and Mantovani, M.S.M., 1995. Description and petrogenesis of the Paraná rhyolites, southern Brazil. Journal of Petrology, 36, 1193-1227.

Goncalves, A.O., Melgarejo, J.C. and Abella, P.A., 2009. Sequence of crystallization of pegmatites: The Angola case. Estudos Geológicos, 19, 35-39.

Harris, C. and Milner, S.C., 1997. Crustal origin for the Paraná rhyolites: Discussion of 'Description and petrogenesis of the Paraná rhyolites, southern Brazil' by Garland et al. (1995). Journal of Petrology, 38, 299-302.

Harris, C., le Roux, P., Cochrane, R., Martin, L., Duncan, A.R., Marsh, J.S., Le Roex, A.P. and Class, C. (2015) The oxygen isotope composition of Karoo and Etendeka picrites: High $\delta 18O$ mantle or crustal contamination ? Contributions to Mineralogy and Petrology, DOI 10.1007/s00410-015-1164-1.

Janasi, V. de A., de Freitas, V.A. and Heaman, L.H., 2011. The onset of flood volcanism, northern Paraná Basin, Brazil: a precise U-Pb baddeleyite/zircon age for a Chapecó-type dacite. Earth and Planetary Science Letters, 302, 147-153.

Lapido Loureiro, F.E. de V., 1973. Carbonatitos de Angola. Memórias e Trabalhos do Instituto de Investigação Cientifica de Angola, 11, 242 pp.

Le Maitre, R.W. 1989. A classification of igneous rocks and glossary of terms – recommendations of the International Union of Geological Sciences Subcommission on the Systematics of Igneous Rocks. Blackwell Scientific, Oxford.

Marques, L.S., Dupré, B. and Picirillo, E.M., 1999. Mantle source compositions of the Paraná Magmatic Province (southern Brazil): Evidence from trace elements and Sr-Nd-Pb isotope geochemistry. Journal of Geodynamics, 28, 429-459.

Marsh, J.S., Ewart, A., Milner, S.C., Duncan, A.R. and Miller, R. McG., 2001. The Etendeka Igneous Province: magma types and their stratigraphic distribution with implications for the evolution of the Paraná-Etendeka flood basalt province. Bulletin of Volcanology, 62, 464-486.

Martin, H., Mathias, M. and Simpson, E.S.W., 1960. The Damaraland sub-volcanic ring complexes in South West Africa. Report, International Geological Congress, Norden, 13, 156-174.

Milner, S.C., Duncan, A.R., Whittingham, A.M. and Ewart, A., 1995. Trans-Atlantic correlation of eruptive sequences and individual silicic units within the Paraná-Etendeka igneous province. Journal of Volcanology and Geothermal Research, 69, 137-157.

Nardy, A.J.R., Machado, F.B. and de Oliveira, M.A.F., 2008. As rochas vulcânicas mesozóicas ácidas da Bacia do Paraná: litoestratigrafia e conciderações geoquímico-estratigráficas. Revista Brasileira de Geociências, 38, 178-195.

Peate, D.W., 1997. The Paraná-Etendeka Province. In: Mahoney, J.J. and Coffin, M.F. (Eds) Large igneous provinces: Continental, oceanic and planetary flood volcanism. Geophysical Monograph, 100, 217-246.

Peate, D.W., Hawkesworth, C.J., Mantovani, M.S.M., Rogers, N.W. and Turner, S.P., 1999. Petrogenesis and stratigraphy of the high Ti/Y Urubici magma type in the Paraná flood basalt province and implications for the 'Dupal'-type mantle in the South Atlantic region. Journal of Petrology, 40, 451-473.

Piccirillo, E.M., Comin-Chiaramonti, P., Bellieni, G., Civetta, L., Marques, L.S., Melfi,, A.J., Petrini., R., Raposo, M.I.B. and Stolfa, D., 1988. Petrogenetic asects of continental flood basalt-rhyolite suites from the Paraná Basin (Brazil). In: Piccirillo, E.M. and Melfi, A.J. (Eds) The Mesozoic Flood Volcanism of the Paraná Basin: Petrogenetic and Geophysical Aspects. São Paulo: Instituto Astronomica e Geofisica Publishers, IAG-USP Press, 179-205.

Piccirillo, E.M.,Bellieni, G., Cavazzini, H., Comin-Chiaromonti, P., Petrini, R., Melfi, A.J., Pinese, J.P.P., Zantadeschi, P. and de Min, A., 1990. Lower Cretaceous tholeiitic dyke swarms in the Ponta Grossa Arch (South East Brazil): Petrology, Sr-Nd isotopes, and genetic relationships with the Paraná flood volcanics. Chemical Geology, 89, 19-48.

Pinto, V.M., Hartmann, L.A., Santos, J.O.S., McNaughton, N.J. and Wildner, W., 2011. Zircon U-Pb geochronology from the Paraná bimodal volcanic province support a brief eruptive cycle at ≈ 135 Ma. Chemical Geology, 281, 93-102.

Renne, P.R., Glen, J.M., Milner, S.C. and Duncan, A.R., 1996. Age of Etendeka flood volcanism and associated intrusions in southwestern Africa. Geology, 24, 659-662.

Rocha-Júnior, E.R.V., Marques, L.S., Babinski, M., Nardy, A.J.R., Figueiredo, A.M.G. and Machado, F.B., 2013. Sr-Nd-Pb isotopic constraints on the nature of the mantle sources involved in the genesis of the high-Ti tholeiites from northern Paraná Continental Flood Basalts (Brazil). Journal of South American Earth Sciences, 46, 9-25.

Thiede, D.S. and Vansconcelos, P.M., 2010. Paraná flood basalts: Rapid extrusion hypothesis confirmed by new $^{40}Ar/^{39}Ar$ results. Geology, 38, 747-750.

Villa, I.M., de Bièvre, P., Holden, N.E. and Renne, P.R., 2015. IUPAC-IUGS recommendation on the half life of ^{87}Rb. Geochimica et Cosmochimica Acta, 164, 382-385.

Woolley, A.R., 2001. Alkaline rocks and carbonatites of the World. Part 3: Africa. The Geological Society Publishing House, Bath, 372 pp.

FIGURE CAPTIONS

Figure 1. Map of distribution outcrops of the Bero Volcanic Complex, SW Angola

Figure 2. TAS classification (Le Maitre, 1989) of Bero mafic and silicic rocks. Dashed lines enclose, with increasing SiO2, fields for mafic, latite and quartz latite compositions in the Etendeka Igneous Province (Marsh et al, 2001, Figure 3).

Figure 3. Geochemical variation in Bero mafic lavas and intrusions compared to compositional fields of the Etendeka low-Ti and high-Ti Khumib types (solid line) and the Paraná high-Ti Urubici, Pitanga, and Parapanema types (dashed line). The Parapanema field includes data for the Ribeira type with which it has a close geochemical affinity. The Khumib field extends to higher Mg# and lower Sr, TiO_2, Zr and Nb (and other incompatible elements) compared to the Urubici field as it includes a high-MgO subset (formed by accumulation of mafic phenocrysts – Ewart et al., 2004a) not known from the Paraná. Mg# = molar % MgO/(MgO+FeO) where FeO is calculated from total Fe assuming $Fe_2O_3/FeO=0.1$

Figure 4. Geochemical variation of Bero quartz latites in comparison with compositions of those from the Etendeka.

Figure 5. Summary of Sr-, Nd- and Pb-isotopes for Bero rocks. Sr- and Nd-isotopic data are initial ratios whereas Pb isotopes are measured ratios. The short bars show the magnitude of the age correction for Th/Pb and U/Pb ratios typical of the quartz latites. Fields for Etendeka and Paraná samples compiled from data in Ewart et al.(2004a, b), Garland et al.(1995), Peate et al.(1999), Marques et al.(1999) and Rocha-Júnior et al.(2013).

Figure 6. Summary of the stratigraphic distribution of various quartz latites in the Bero complex at different localities. The stratigraphic columns are schematic and not to scale. A summary of the volcanic stratigraphy in the northern Etendeka (Marsh, et al., 2001) is also provided.

Table

Click here to download Table: Table 1.xls

Table 1: Selected major, trace and isotopic analyses of Bero mafic rocks and quartz latites

	Mafic rocks				Quartz latites															
SAMPLE	NBA-36	NBA-61	NBA-117	NBA-139	NBA-45	NBA-108	NBA-118	NBA-57	NBA-115	NBA-90	NBA-124	NBA-58	NBA-130	NBA-74	NBA-68	NBA-62	NBA-91	NBA-112	NBA-72	NBA-127
Type	basalt	mafic dyke	gabbro sheet	evolved gabbro	High Nb			Chinguau				Ventura				Sarusas			Khoraseb	
SiO_2 %	48.68	51.33	48.82	57.21	64.66	66.13	65.55	68.13	67.9	65.97	64.68	63.26	63.16	63.42	62.76	65.31	64.37	63.45	64.5	65.52
TiO_2	3.59	2.67	3.59	1.83	1.07	1.073	1.076	0.772	0.914	0.907	0.9	1.45	1.436	1.45	1.396	1.3	1.25	1.297	1.15	1.18
Al_2O_3	13.19	12.91	13.25	12.59	14.58	14.85	15	12.71	13.29	12.84	12.77	13.68	13.44	13.48	13.78	13.5	12.9	13.47	12.81	13.11
FeO	12.81	11.86	13.02	11.31	3.87	3.81	3.62	4.18	5.56	5.26	5.22	5.81	6.13	6.05	6.05	5.06	6.73	7.18	6.18	6.07
MnO	0.17	0.29	0.18	0.17	0.1	0.11	0.101	0.06	0.1	0.12	0.12	0.09	0.14	0.09	0.123	0.07	0.12	0.22	0.12	0.1
MgO	4.99	5.17	5.1	1.52	0.882	0.926	0.82	0.84	1.29	0.75	0.78	0.78	1.4	1.11	1.47	0.79	1.47	1.93	1.47	1.17
CaO	8.88	9.29	8.77	4.71	2.02	1.48	2.2	1.52	1.85	2.47	2.49	2.65	3.02	2.58	2.94	2.63	2.43	2.37	2.03	2.35
Na_2O	2.62	2.32	2.38	2.74	4.35	3.43	4.26	2.58	2.68	3.4	3.66	3.12	3.05	3.35	3.15	3.06	2.84	2.79	3.04	2.93
K_2O	1.41	0.93	1.39	3.31	5.65	7.28	5.63	5.13	4.59	3.64	3.24	4.86	4.42	4.51	4.56	4.44	4.20	3.97	4.29	4.70
P_2O_5	0.47	0.33	0.50	0.68	0.22	0.24	0.23	0.19	0.24	0.23	0.24	0.46	0.47	0.44	0.44	0.39	0.38	0.41	0.31	0.32
LOI	3.12	2.67	2.31	3.02	1.81	1.08	1.74	2.95	1.53	3.38	3.65	2.62	2.59	1.70	3.16	3.11	2.47	2.02	1.93	2.70
H_2O-	nd	0.54	0.54	0.66	0.39	0.21	0.33	1.14	0.65	0.22	0.78	0.80	0.58	0.64	0.55	0.80	0.05	0.82	0.71	0.55
Total	99.94	100.30	99.86	99.75	99.60	100.62	100.56	100.20	100.59	99.19	98.53	99.58	99.83	98.82	100.37	100.46	99.21	99.93	98.54	100.70
XRF trace elements																				
Nb ppm	28	18.9	27	55	104	102	104	51	50	53	52	64	61	60	61	56	53	56	57	57
Zr	245	219	237	548	639	639	639	481	469	481	480	567	560	568	548	576	557	580	564	571
Y	35	47	36.3	69.1	52	53	53	50	52	53	53	51	55	52	55	61	60	65	58	60
Sr	664	278	663	505	154	132	161	208	266	286	319	457	487	550	497	381	371	404	327	313
Rb	26	15	30	85	178	216	178	165	149	144	124	134	126	127	124	114	108	110	129	134
Th	3.5	4.4	<2.5	8.4	20	23	21	18	19	18	19	12	13	12	11	9	10	13	13	14
Pb	5.1	9.8	3.4	10	17	19	16	20	20	38	21	14	19	17	14	15	13	10	17	17
Ba	639	449	590	1131	1061	1023	1103	1496	1462	1386	1424	1248	1395	1922	1213	1024	1086	986	1094	1344
Sc	26	36	26	13	7	7	7	12	16	12	12	14	13	13	13	17	16	18	15	15
Zn	126	136	125	164	70	74	53	70	74	178	94	92	109	111	114	69	102	146	94	100
Cu	156	256	121	167	6	17	7	13	11	17	14	14	12	12	12	39	10	9	16	11
Ni	77	45	72	<3	12	10	7	7	6	6	4	6	5	7	6	6	6	3	6	4
Co	43	47	48	14	2.5	5	<2.5	4	6	5	<2.5	6	8	3	5	4	5	6	3	6
Cr	68	70	58	<3	26	16	15	11	6	9	5	11	4	8	9	9	11	8	10	5
V	414	430	439	22	38	33	35	13	11	15	10	40	41	32	35	30	15	15	17	18
La	32	22	nd	nd	94	80	93	77	75	78	nd	80	80	79	80	68	64	64	73	nd
Ce	82	61	nd	nd	178	189	193	156	161	157	nd	164	176	169	170	152	144	150	155	nd
Nd	32	34	nd	nd	75	70	77	71	71	73	nd	80	81	82	83	77	74	73	73	nd
ICP-MS trace elements																				
La ppm	31.1		31.5		88.7	79.8	93.4	63.8	74.7	71.8	74.4	76.3	80.1	78.8	76.9	68.7	65.0	63.8	70.6	
Ce	72.1		72.4		185	189	193	141	161	156	159	166	176	170	169	158	145	150	158	
Pr	9.47		9.53		19.6	19.5	21.7	15.4	18.7	17.3	18.4	19.2	20.8	20.7	19.4	19.2	17.2	17.9	18.1	
Nd	40.8		41.3		77	69.8	77	68.7	70.9	70.1	69.6	79.8	81.5	81.1	80.9	78	72.9	73.1	75.6	
Sm	8.92		8.94		12	12	13.2	10.5	13.0	12.1	12.8	14.0	15.3	15.3	14.6	15.9	14.2	14.9	14.1	
Eu	2.67		2.77		2.49	2.40	2.70	2.42	3.04	2.88	3.00	3.44	3.67	3.62	3.65	3.80	3.58	3.87	3.27	
Gd	8.05		8.18		9.29	9.25	10.17	8.61	10.6	10.2	10.7	11.4	12.4	12.0	12.2	13.3	12.5	13.0	12.0	
Tb	1.12		1.12		1.33	1.35	1.47	1.20	1.52	1.41	1.52	1.50	1.70	1.67	1.64	1.87	1.70	1.89	1.66	
Dy	6.51		6.57		8.29	8.19	8.96	7.35	9.13	8.80	9.17	8.91	9.75	9.71	9.74	11.1	10.6	11.6	10.1	
Ho	1.16		1.17		1.54	1.53	1.68	1.39	1.69	1.63	1.69	1.58	1.75	1.74	1.75	2.02	1.93	2.10	1.84	
Er	3.11		3.10		4.49	4.46	4.79	3.98	4.79	4.59	4.83	4.29	4.73	4.72	4.69	5.58	5.38	5.77	5.15	
Tm	0.398		0.396		0.647	0.637	0.678	0.553	0.66	0.64	0.658	0.577	0.625	0.632	0.620	0.751	0.721	0.756	0.691	
Yb	2.50		2.48		4.29	4.29	4.58	3.66	4.38	4.18	4.37	3.67	4.02	4.12	3.96	4.84	4.69	4.92	4.49	
Lu	0.360		0.366		0.632	0.647	0.687	0.527	0.657	0.594	0.663	0.512	0.594	0.600	0.550	0.710	0.649	0.703	0.625	
Hf	5.88		5.73		13.5	14.2	14.7	10.5	11.6	10.6	11.2	12.3	13.2	13.4	12.2	14.2	12.3	8.81	12.6	
Ta	1.47		1.45		3.90	4.48	4.48	2.07	2.47	2.08	2.40	2.55	2.97	3.05	2.52	2.78	2.21	2.64	2.35	
Pb	4.64		4.00		16.6	15.8	15.2	20.5	22.5	34.3	20.2	15.7	17.2	16.7	15.3	15.3	12.6	8.87	16.8	
Th	2.76		2.89		17.2	16.3	18.0	15.2	16.0	15.4	15.8	11.9	11.8	12.3	11.4	10.3	9.60	9.51	12.1	
U	0.593		0.601		3.31	3.81	3.27	3.23	3.46	3.42	3.45	3.12	2.69	2.60	2.67	3.93	2.55	2.12	2.76	
Isotopes																				
$^{87}Sr/^{86}Sr$	.705797±12		.705900±15		.715053±13	.717377±15	.714563±12	.718540±11	.716049±13	.715883±14	.715167±13	.709293±14	.708447±12	.708745±16	.708371±11	.708156±14	.708066±12	.708038±14	.710229±14	
$^{143}Nd/^{144}Nd$	.512436±11		.512432±12		.512291±12	.512285±10	.512290±8	.512069±13	.512118±10	.512098±11	.512100±8	.512333±10	.512339±7	.512336±12	.512343±10	.512401±8	.512394±12	.512403±10	.512337±11	
$^{206}Pb/^{204}Pb$	18.123±1		18.204±1		18.600±1	18.659±1	18.649±1	19.045±1	18.998±1	18.899±1	18.991±1	18.504±1	18.415±1	18.553±1	18.457±1	18.871±1	18.563±1	18.536±1	18.545±1	
$^{207}Pb/^{204}Pb$	15.561±1		15.577±1		15.671±1	15.672±1	15.670±1	15.749±1	15.739±1	15.734±1	15.737±1	15.625±1	15.624±1	15.645±1	15.621±1	15.680±1	15.633±1	15.634±1	15.642±1	
$^{208}Pb/^{204}Pb$	38.498±3		38.618±4		39.179±2	39.234±3	39.249±4	39.547±2	39.472±4	39.331±2	39.449±4	38.791±3	38.745±4	38.897±3	38.814±3	38.896±4	38.856±3	38.931±2	38.879±2	
$(^{87}Sr/^{86}Sr)_i$	0.70558		0.70565		0.70876	0.70846	0.70854	0.71422	0.7123	0.71314	0.71305	0.7077	0.70704	0.70749	0.70701	0.70653	0.70648	0.70656	0.708082	
$(^{143}Nd/^{144}Nd)_i$	0.51232		0.51232		0.51221	0.51219	0.5122	0.51199	0.51202	0.51201	0.512	0.51224	0.51224	0.51224	0.51225	0.51229	0.51229	0.5123	0.51224	
epsilon Nd_i	-2.83		-2.88		-5.01	-5.3	-5.19	-9.31	-8.67	-8.95	-9.03	-4.4	-4.41	-4.47	-4.25	-3.36	-3.41	-3.32	-4.43	
$(^{206}Pb/^{204}Pb)_i$	17.953		18.003		18.33	18.332	18.357	18.829	18.788	18.323	18.757	18.236	18.205	18.343	18.248	18.522	18.29	18.24	18.323	
$(^{207}Pb/^{204}Pb)_i$	15.553		15.567		15.658	15.656	15.656	15.738	15.729	15.631	15.726	15.612	15.614	15.635	15.611	15.663	15.62	15.618	15.631	
$(^{208}Pb/^{204}Pb)_i$	38.238		38.302		38.719	38.775	38.723	39.214	39.153	38.56	39.098	38.457	38.442	38.572	38.486	38.597	38.52	38.457	38.56	

<n - lower than the detection limit of 'n'
nd - not determined

Table
Click here to download Table: Table 2.xlsx

Table 2: Mean and standard deviation of some interelement ratios and ranges for isotopic ratiosfor Be

Type	Locality	Ti/Y	Ce/Pb	La/Yb	Zr/Nb	Eu/Eu*
Sarusas	Etendeka	123±15	13.9±1.9	13.0	11.5±0.4	0.82
	Bero (10)	121±8	12.9±3.4	13.7	10.4±0.2	0.82
Ventura	Etendeka	188±22	11.1±0.8	25.5	9.2±0.1	0.82
	Bero (10)	159±10	10.5±0.4	19.9	9.2±0.2	0.82
Khoraseb	Etendeka	124±11	10.2±1.1	15.8±0.8	10.8±0.5	0.76±.01
	Bero (3)	117	9.6	15.3	10	0.77
High Nb	Bero (5)	123±2	12.0±0.8	19.9	6.2±0.1	0.71
Chinguau	Bero (10)	107±15	7.3±0.5	17.2	9.1±0.2	0.78
Low-Ti Quartz latites						
Awahab	S Etendeka	125±5	4.1±0.5	10.9±0.5	12.9±0.7	0.65±0.03
Fria	N Etendeka	78±9	3.7±0.6	11	11.5±0.7	0.59
Beacon	S Etendeka (1	133±8	4.4±0.6	9	12.4±0.7	0.71

Etendeka data from Ewart et al. (2004), Ewart et al.(1998) and Marsh et al.(2001)
Ti/Y, Ce/Pb, Zr/Nb, Rb/Sr calculated from XRF data; La/Yb and Eu/Eu* from ICP-MS data
Standard deviations given where data for 5 samples or more are available
(n) - number of samples